Bull. Mater. Sci., Vol. 36, No. 6, November 2013, pp. 1043–1048. © Indian Academy of Sciences.

Zirconium influence on microstructure of aluminide coatings deposited on nickel substrate by CVD method

JOLANTA ROMANOWSKA*, MARYANA ZAGULA-YAVORSKA and JAN SIENIAWSKI
Department of Materials Science, Rzeszów University of Technology, 2, W. Pola st, 35-958 Rzeszów, Poland

MS received 30 May 2012; revised 18 September 2012

Abstract. **Influence of Zr on the microstructure and phase characteristics of aluminide diffusion coatings deposited on the nickel substrate has been investigated in this study. The coatings with and without zirconium were deposited by CVD method. The cross-section chemical composition investigations revealed that during the coatings formation, there is an inward aluminum diffusion and outward nickel diffusion in both types of coatings (with and without zirconium), whereas zirconium is located far below the coating surface, at a depth of ∼17 μm, between β-NiAl phase and γ'-Ni_3Al phase. XRD examinations showed that β-NiAl, γ-NiAl and γ'-Ni_3Al were the main components of the deposited coatings. β-NiAl phase is on the surface of the coatings, whereas γ-NiAl and γ'-Ni_3Al form deeper parts of the coatings. Zirconium is dissolved in NiAl on the border between β-NiAl and γ'-Ni_3Al.**

Keywords. **Aluminides; nickel; zirconium; diffusion; CVD.**

1. Introduction

Turbine blades in aerospace turbine engines, exposed to oxidation at high temperature (above 1100 °C) are protected by alumina coatings such as nickel aluminide. High temperature coatings based on β-NiAl intermatallic phase are extensively used to protect components against oxidation in gas turbine engines. However, aluminide coatings based on NiAl phase do not fulfil the requirements such as good adhesion of the oxide scale on NiAl layer and long oxidation resistance at high temperature (Loira 2000, 2001).

Modification of the aluminide coatings by platinum is the most effective way to increase oxidation resistance of the turbine blades (Angete and Stiller 2001; Purvis and Warnes 2001; Wang and Sayre 2009). The adhesion of the oxide scale on NiAl layer is a key issue to determine lifetime of the blades. Platinum accelerates the formation of thermally stable oxide Al_2O_3 and improves the oxide scale adherence (Yavorska *et al* 2012), reduces voids formation at the interface of metal/oxide (Pezdra *et al* 2009). Platinum modification of aluminide coatings improves the stability of β-NiAl phase and delays the transformation of β-NiAl to γ'-Ni_3Al phase. Platinum accelerates aluminum diffusion, reduces the flux of vacancies from the metal to the surface and inhibits vacancy coalescence and internal voids formation, decreases the diffusion of alloying elements to the coating, promotes a selective alumina scale formation and accelerates healing after spallation (Niu *et al* 1993). In industry, Pt-modified NiAl coatings are used, but other systems are being investigated to replace them (Hamadi *et al* 2009; Pint *et al* 2010; Wang *et al* 2011). Addition of small amounts of reactive elements, such as Zr, Hf, Y or Ce to NiAl samples has beneficial effects on oxidation behaviour. This beneficial effects include an improvement in the adhesion of alumina scales and reduction of oxide scale growth rate (Pint *et al* 2010). Research on Hf-doped cast alloys (Wang *et al* 2011) indicated Hf doping of β-NiAl and Ni–Pt aluminides reduces the parabolic rate constant by a factor of ten and even possibly to be more efficient than Pt addition. It was found that Hf-rich precipitated particles were observed mainly close to the coating surface, along grain boundaries, and at the interface between the additive layer and the inter-diffusion layer. This is expected to be due to Hf low solubility and low diffusivity in β-NiAl coating phase. The interface corresponds to the initial surface of the substrate. Hf-rich particles at the interface indicate that Hf deposition occurs at the beginning of the vapour phase aluminizing deposition process. As Hf-rich particles were observed at the surface, along grain boundaries and at the interface between the additive layer and the inter-diffusion layer, Wang *et al* (2011) assumed that β-NiAl phase is saturated with Hf at the coating process. Zirconium influences the initial stages of oxide growth and accelerates the transition between the transient and stationary regimes of oxidation. Zirconium co-deposited with aluminum on the nickel superalloy by CVD process developed by Onera and Snecma, in which Zr is provided by $Zr_0Cl_2{\cdot}8H_2O$ activator (Hamadi *et al* 2009), locates far below the coating surface, at the interface between β-NiAl coating and the inter-diffusion zone. This interface corresponds to the initial surface of the superalloy and zirconium deposition occurs at the beginning of the process. The inter-diffusion zone consists of β-NiAl matrix and phases containing additional elements from the superalloy (Cr, Co, W, Al, Ti and Mo) (Hamadi *et al* 2009). During oxidation, zirconium migrates towards the surface

*Author for correspondence (jroman@prz.edu.pl)

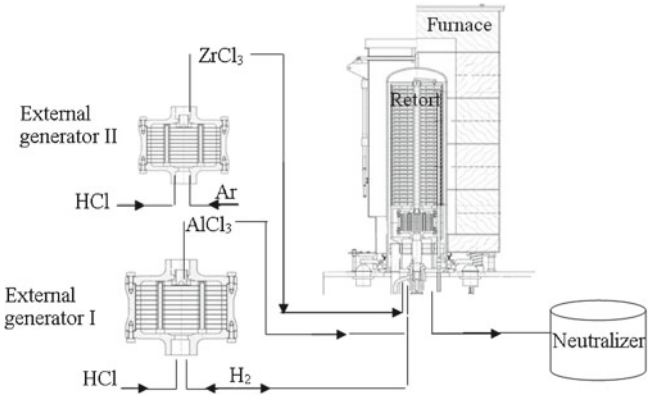

Figure 1. Equipment for CVD method.

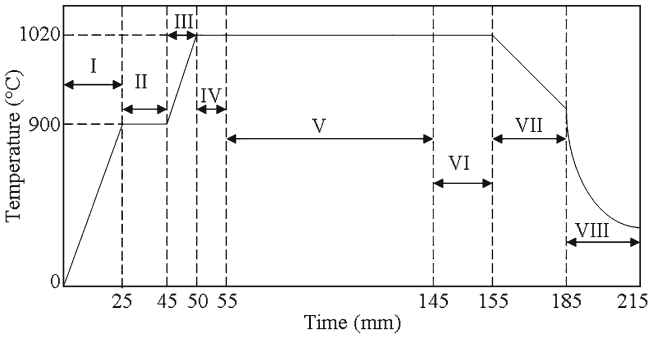

Figure 2. Temperature profile of CVD process.

and Zr distribution in the whole oxide layer becomes homogeneous. Zr may migrate via NiAl grain boundaries, where it is known to segregate (Larson and Miller 2000). Thus, Zr present in the oxide can be expected to modify the stress relief by reducing the oxide creep rate. Zirconium delays the oxide-scale spalling and inhibits the formation of cavities at the metal/oxide interface and there is no voiding at the metal/oxide interface, unlike in Pt-modified NiAl coatings. The absence of voiding in the presence of Zr is expected to improve thermally grown alumina adhesion on the nickel aluminide (Hamadi *et al* 2009).

In this paper, influence of zirconium on the microstructure and phase composition of aluminide diffusion coatings deposited on the nickel substrate by CVD method is analysed. The microstructure, phase composition and elements' distribution of coatings with and without zirconium are compared.

2. Experimental

The commercial nickel of 99·95 wt% purity was used in this study. The cylindrical samples of 20 mm diameter and 4 mm high were cut and ground up to SiC no. 1000, degreased in ethanol, ultrasonically cleaned and finally aluminized.

The aluminide coatings were made using CVD equipment BPXPR0325S manufactured by IonBond company (figure 1)

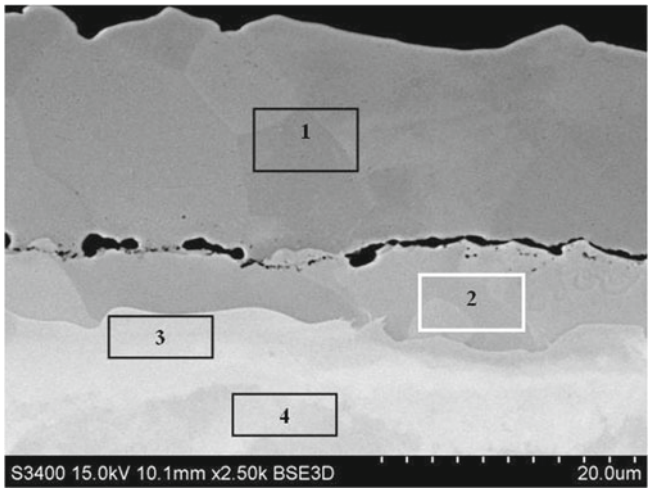

Figure 3. Microstructure of coating on pure nickel.

Table 1. Electron probe microanalysis, figure 3 (wt%).

Points	Al	Ni
1	23·01	76·99
2	12·97	87·03
3	6·26	93·74
4	–	100·00

(Zielińska *et al* 2011). The aluminizing process was performed in two ways. In the first one, the aluminizing process was conducted for 4 h at a temperature of 1000 °C. Aluminum chloride vapour ($AlCl_3$) was produced in an external generator I (figure 1) at 330 °C according to the reaction:

$$2Al + 6HCl \rightarrow 2AlCl_3 + 3H_2.$$

Then the saturating atmosphere was transported in a stream of hydrogen gas into CVD reactor, where nickel samples were placed. $AlCl_3$ vapour reacted with the nickel at a temperature of 1000 °C and grains of intermetallic phase NiAl were formed according to the reaction:

$$2AlCl_3 + 2Ni + 3H_2 \rightarrow 2AlNi + 6HCl.$$

The second way of aluminizing process consists of the following steps (figure 2): heating from room temperature up to 900 °C; aluminizing at 900 °C for 20 min; heating from 900 to 1020 °C; aluminizing at 1020 °C for 5 min; aluminizing and zirconizing at 1020 °C for 90 min; aluminizing at 1020 °C for 10 min; cooling samples with furnace to 500 °C; and cooling samples in air atmosphere.

Zirconium chloride vapour ($ZrCl_3$) was produced in an external generator II (figure 1) at 440 °C according to the reaction:

$$2Zr + 6HCl \rightarrow 2ZrCl_3 + 3H_2.$$

The saturation atmosphere was transported in a stream of hydrogen gas into CVD reactor, where nickel samples were

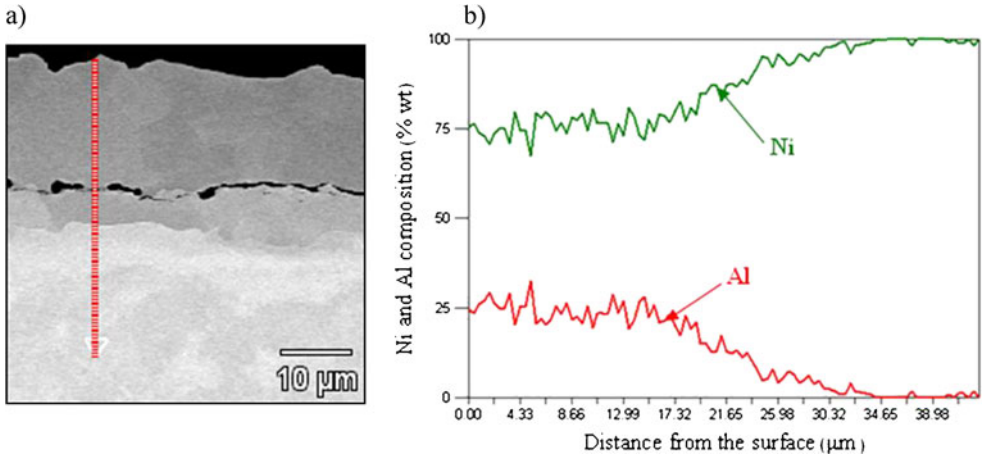

Figure 4. EDS analyses of aluminide coatings.

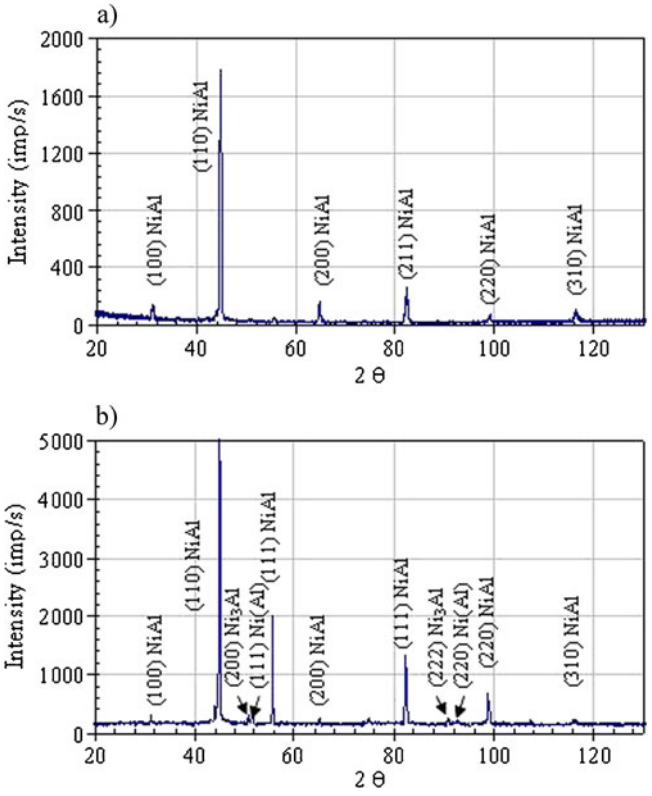

Figure 5. XRD phase analyses of alumina coatings.

placed. $AlCl_3$ and $ZrCl_3$ vapours reacted with nickel at 1020 °C and an intermetallic phase NiAl(Zr) was formed according to the reaction:

$$AlCl_3 + ZrCl_3 + Ni + 3H_2 \rightarrow NiAl(Zr) + 6HCl.$$

Zirconium doping aluminizing process was described by Bacos *et al* (2011), but our process is different from the process presented in Bacos *et al* (2011). In both processes, Zr and Al are co-deposited on the substrate, but in Onera and Snecma process, Zr is provided by $ZrOCl_2$ activator, whereas in the process described in this work, it is by $ZrCl_3$.

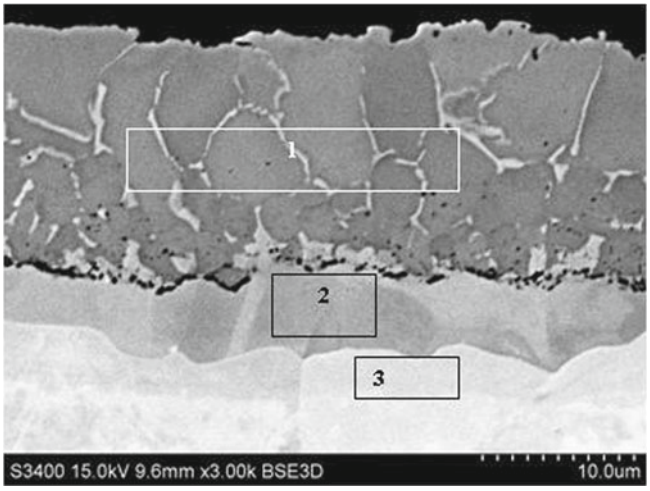

Figure 6. Zirconium-doped coating microstructure.

The microstructure of the cross-sections of the coatings were investigated by an optical microscope Nikon Epiphot 300, scanning electron microscope (SEM) Hitachi S-3400N and energy dispersive spectroscope (EDS) (Pint *et al* 2010; Zielińska *et al* 2011). The coatings thicknesses were determined by means of NIS–Elements software. Eight measurements for each sample were performed.

Phase composition of the coatings was investigated using ARL X'TRA X-ray diffractometer, equipped with a filtered copper lamp with a voltage of 45 kV.

3. Results

SEM investigation and EDS analysis of aluminide coatings on pure nickel revealed their triple-zone structure (figure 3, table 1). In the first zone, on the top of coating, the proportion of Ni to Al corresponds to β-NiAl phase (table 1, point 1). The thickness of the top-zone is about 18 μm. The second zone, below is thinner (about 7 μm) and consists of γ'-Ni_3Al phase (table 1, point 2). The chemical composition

Table 2. Electron probe microanalysis, figure 6 (wt%).

Points	Al	Ni
1	23·27	76·73
2	11·97	88·03
3	2·73	97·27

Table 3. Electron probe microanalysis, figure 7 (wt%).

Points	Al	Ni	Zr
1	14·19	85·81	–
2	15·0	85·0	–
3	17·45	82·55	–
4	15·77	82·75	1·48

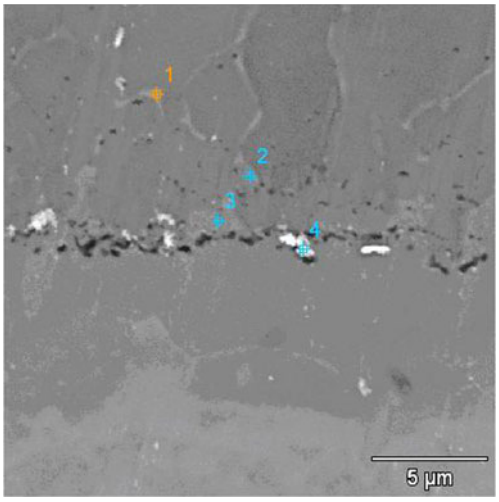

Figure 7. Layers' microstructure.

of the third, inner zone, corresponds to γ-Ni(Al) phase, i.e. the aluminum solid solution in nickel (table 1, point 3). Chemical composition of the zone below γ-Ni(Al) phase is same as the matrix composition that is pure nickel (table 1, point 4).

EDS analysis of the cross-section of the aluminide coating and the concentration profiles (figure 4(a and b)) confirmed nickel outward diffusion from the substrate and aluminum inward diffusion from the surface. The decrease of aluminum content and increase of nickel content from the surface to the material substrate is typical of the low-activity aluminizing process. XRD surface analysis of the nickel sample with aluminide coating indicated only the existence of β-NiAl phase (figure 5a), while results of XRD analysis inside the aluminide coating revealed the presence of three phases: β-NiAl, γ'-Ni_3Al and γ-Ni(Al) (figure 5b).

SEM investigation and EDS analysis of the zirconium-doped aluminide coating on the pure nickel revealed the existence of the same, triple zone structure, identical with coatings without zirconium (figure 6), i.e. β-NiAl (point 1, table 2), γ'-Ni_3Al (point 2, table 2) and γ-Ni(Al) point 3, table 2). Zirconium was found in 'inclusions' between β-NiAl and γ'-Ni_3Al layers, 17 μm from the coating's surface (figure 7, table 3). Zirconium content in these

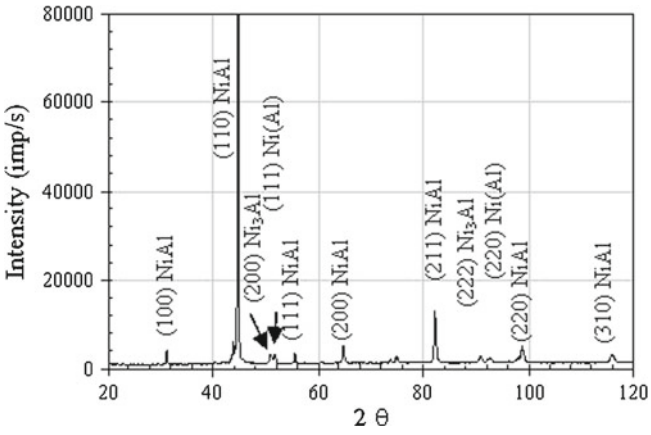

Figure 9. XRD analysis of zirconium doped coating.

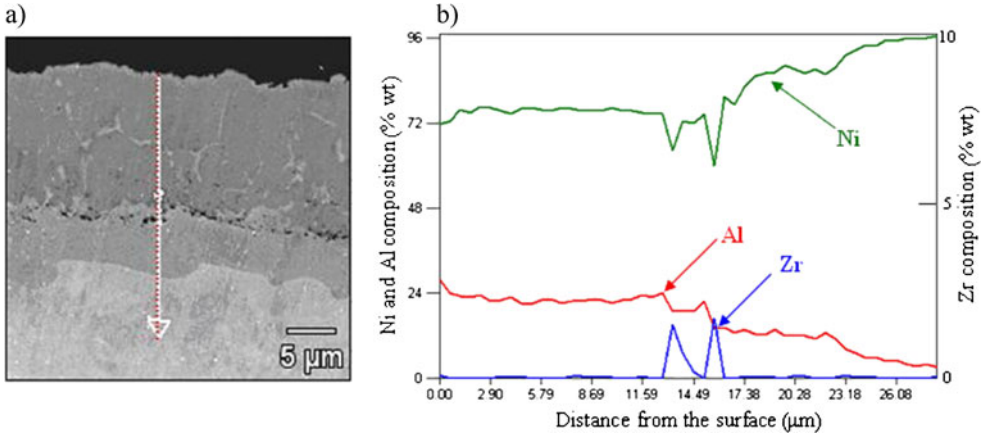

Figure 8. EDS analyses of zirconium doped coatings.

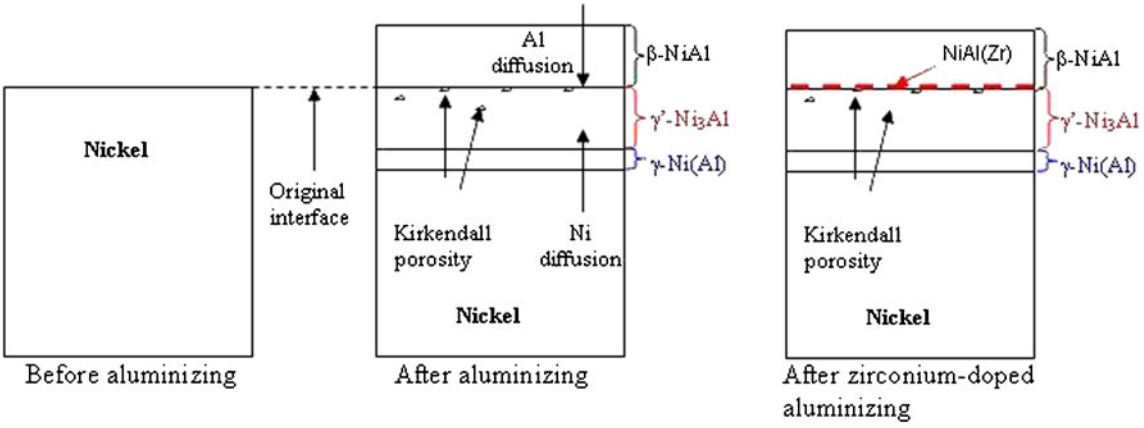

Figure 10. Diffusion coatings on pure nickel.

'inclusions' is 1·48 wt% (0·79 at%) (figure 7, point 4). Similar results were obtained for zirconium-doped aluminide coating deposited by the vapour phase at 1100 °C for 5 h on nickel-based AM1 superalloy by Hamadi *et al* (2009). In these inclusions, according to Bozzolo *et al* (2000), zirconium atoms prefer to occupy places in aluminum sublattice in NiAl phase and form NiAl(Zr) phase. Microstructure analysis of the top layer of zirconium-doped aluminide coatings revealed the intermetallic phases distributed on the grain boundaries of β-NiAl phase. The chemical composition of those phases corresponds to γ'-Ni_3Al phase (figure 7, point 1–3, table 3).

EDS analysis and concentration profiles of the cross-section of the analysed coatings (with and without zirconium) showed outward nickel diffusion from the substrate and the inward aluminum diffusion from the surface to the nickel substrate (figures 4 and 8). During aluminizing process, nickel preferentially diffuses out through the coating and combines with aluminum to form β-NiAl, γ'-Ni_3Al and γ-Ni(Al) phases. The coating grows outward. As the outward diffusion of nickel is faster than the inward diffusion of aluminum, Kirkendall porosity is generated below the original interface (figure 9). Kirkendall porosity forms in some systems because of unbalanced diffusion of species into and out of the alloy. The area of significant porosity is formed between inward and outward zones of aluminide coating. According to Kirkendall–Frenkel theory, there is an unbalanced flow of nickel and aluminum atoms in the diffusion zone. The value of nickel diffusion coefficient is bigger than aluminum diffusion coefficient ($D_{Ni} > D_{Al}$). The unbalanced flux of nickel and aluminum atoms results in the differences in microvolume and causes stress in the diffusion zone. The microvolume is reduced in the area of higher nickel concentration and vacancies are formed. When the number of vacancies are big, vacancies coagulate and this way pores are being formed. This way Kirkendall porosity is generated.

During zirconium-doped aluminizing, aluminum diffuses inward, to the nickel substrate, zirconium diffuses to β-NiAl/γ'-Ni_3Al layers' border, where Zr atoms substitute for Al atoms in the β-NiAl phase (Bozzolo *et al* 2000).

XRD surface analysis of nickel sample with zirconium-doped aluminide coating indicated only the existence of same phases as in the case of coatings without zirconium, i.e. the β-NiAl, γ'-Ni_3Al and γ-Ni(Al) phases (figure 9).

4. Conclusions

This paper presents the results of microstructure analysis of the aluminide coatings with and without zirconium deposited on the pure nickel by CVD method. The structure of both kinds of coatings are the same: the top β-NiAl zone, the middle γ'-Ni_3Al zone and the inner γ-Ni(Al) zone. In the zirconium-doped coating, zirconium is in 'inclusions' of NiAl(Zr) phase containing 1·48 wt% zirconium. NiAl(Zr) phase is β-NiAl phase, in which Zr atoms substitute for Al atoms. This phase is located far below the coating surface, at the interface between β-NiAl and γ'-Ni_3Al phases. Moreover, the γ'-Ni_3Al phase was found along grain boundaries in β-NiAl phase in the zirconium-doped coating. The analysed coatings were formed through the nickel outward diffusion from the substrate and the aluminum inward diffusion from the surface to the nickel substrate. Zirconium diffused from the surface to β-NiAl/γ'-Ni_3Al layers' border, where it was incorporated in to the β-NiAl lattice (figure 10).

Acknowledgement

The present research was supported by the National Science Centre, Poland (project number UMO-2011/01/DST8/05/036).

References

Angete J and Stiller K 2001 *Mater. Sci. Eng.* **A316** 182

Bacos M, Dorvaux J, Landais S, Lavigne O, Mevrel R, Poulain M, Rio C and Vidal-Setif M 2011 *The Onera Journal Aerospace Lab.* **3** 1

Bozzolo G, Noebe R and Honecy F 2000 *Intermetallics* **8** 7

Hamadi S, Bacos M P, Poulain M, Seyeux A, Maurice V and Marcus P 2009 *Surf. Coat. Technol.* **204** 756

Larson D J and Miller M K 2000 *Mater. Charact.* **44** 159
Loira E 2000 *Intermetallics* **8** 1339
Loira E 2001 *Intermetallics* **9** 997
Niu Y, Wu W, Boone D, Smith J, Zhang J and Zhen C 1993 *J. Phys.* **IV** 511
Pezdra Z, Kennedy A, Kopecek J and Moretto P 2009 *Surf. Coat. Technol.* **200** 4032
Pint B A, Haynes T M and Besmann T M 2010 *Surf. Coat. Technol.* **205** 3287
Purvis A L and Warnes B M 2001 *Surf. Coat. Technol.* **146–147** 1
Wang Y and Sayre G 2009 *Surf. Coat. Technol.* **203** 1264
Wang Y, Suneson M and Sayre G 2011 *Surf. Coat. Technol.* **206** 1218
Yavorska M, Sieniawski J, Filip R and Gancarczyk T 2012 *Adv. Mater. Res.* **49** 883
Zielińska M, Sieniawski J, Yavorska M and Motyka M 2011 *Arch. Metal. Mater.* **56** 185